SATELLITE & MESOMETEOROLOGY RESEARCH PROJECT

Department of the Geophysical Sciences
The University of Chicago

RAWINSONDE DETECTION OF STRATOSPHERIC MOISTURE IN THE VICINITY OF THUNDERSTORM TOPS

Peter D. McGurk

SMRP Research Paper 176
June 1979

RAWINSONDE DETECTION OF STRATOSPHERIC MOISTURE IN THE VICINITY OF THUNDERSTORM TOPS

Peter D. McGurk
Department of the Geophysical Sciences
The University of Chicago

SMRP Research Paper No. 176
June 1979

Rawinsonde Detection of Stratospheric Moisture in the Vicinity of Thunderstorm Tops

Peter D. McGurk

Abstract

During May and June, 1978, close to 200 soundings were taken at Yorkville, Illinois for Project NIMROD. Many of these ascents were tracked well into the lower stratosphere to their burst and descent back into the troposphere. Soundings taken during a severe thunderstorm over Northern Illinois on June 16, 1978 detected humidity in the stratosphere a few kilometers above the storm top. The location of the radiosondes in relation to the thunderstorms was determined by using a sequence of satellite pictures. The overshooting and collapsing processes atop severe thunderstorms are suggested as a mechanism for the moisture transport.

1. INTRODUCTION

In May, 1978, Project NIMROD (Northern Illinois Meteorological Research On Downbursts) went into full operation. Under the direction of Prof. T. Theodore Fujita, meteorologists from the National Center for Atmospheric Research (NCAR), the National Weather Service (NWS), the Illinois State Water Survey (ISWS), and the University of Chicago operated an extensive mesometeorological network in the Chicago area. Data were collected on 20 operational days through June 1978. The Project was undertaken to obtain a better understanding of thunderstorms which produce damaging winds on the ground.

A map of the NIMROD Network is presented in Fig. 1. Three Doppler radars were used to measure reflectivity and wind velocity, scanning storms every 3 minutes. The NCAR radars located at Yorkville, Illinois and O'Hare Airport

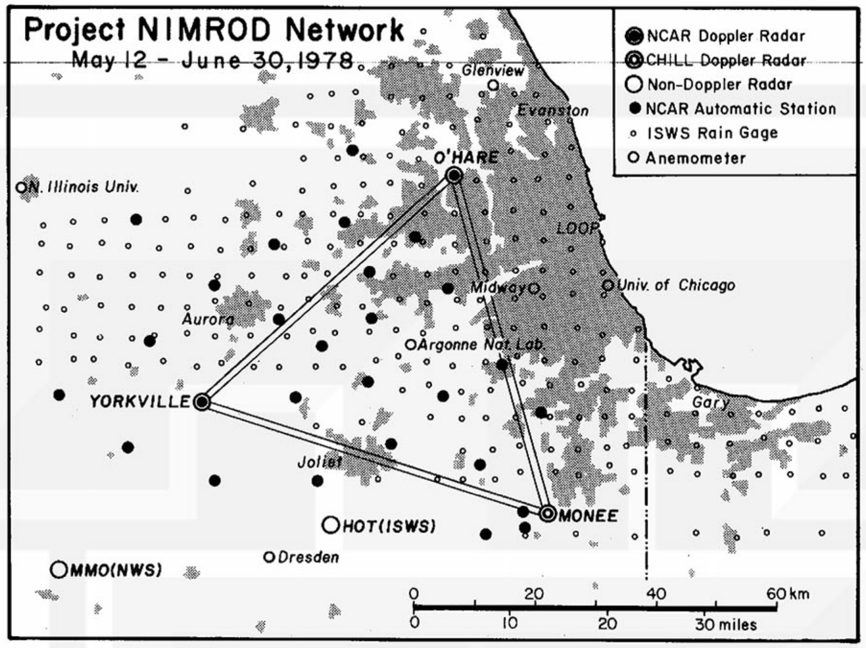

Fig. 1. A map of the NIMROD Network

operated at 5.5 cm wavelengths. The third radar, CHILL from ISWS, had both 3 cm and 10 cm capabilities. In addition, 2 conventional radars were used for general storm surveillance and Doppler scan coordination. These were the NWS WSR-57 radar at Marseilles, Illinois and the ISWS HOT radar located south of Joliet, Illinois. Surface observations were taken using 27 PAM (Portable Automated Meso-network) stations. These stations measured various parameters including wind direction, wind speed, air temperature, surface pressure, and rainfall (Brock and Govind, 1977). Along with the PAM system a dense array of weighing bucket rain-gauges were operated by ISWS. Upper air observations, 193 in all, were taken from Yorkville by NWS operators, with assistance from the University of Chicago, using the AN/GMD-1 rawinsonde system.

The research described in this paper concerns the examination of a portion of the upper-air data, with particular attention to humidity detection near the thunderstorm top. The collapse of overshooting tops will be suggested as a mecha-nism for this moisture transport.

2. SERIAL RAWINSONDE ASCENT OF MAY 29, 1978

Several other mesoscale research projects have incorporated rawinsonde networks into their data collection. The Thunderstorm Project (Byers and Braham, 1949) operated a very dense upper-air network in Florida and Ohio during the late 40s. Simultaneous releases were made by 10 stations at about 2-hour intervals. In April and May, 1965, a rawinsonde network was used by Kreitzberg (1968) to study extratropical cyclones in Project Stormy Spring. Serial soundings were taken at 90-minute intervals from 6 Air Force sites in southern New England. In addition, four Weather Service Offices took special 3-hour soundings in support of the Project. In 1966, NSSL began serial rawinsonde ascents with their mesonetwork in Oklahoma. Ten stations, spaced about 85 km apart, took soundings at 90-minute intervals (Fankhauser, 1974).

Project NIMROD chose to maximize time resolution for the soundings taken at its one upper-air station. Hourly and half-hourly releases were made throughout the periods of severe weather. When launches were spaced 60 minutes apart, it was possible to track many of the radiosondes to the point where the balloon burst in the stratosphere. Then, these same units were followed for as long as possible as they descended through the lower stratosphere and back into the troposphere. In light of the well-known tracking errors with the GMD-1 system at low-elevation angles, winds were not computed below 10 km elevation. Nevertheless, notice how well the winds compare on the ascending and descending portions of the same flight.

A typical serial ascent is that of May 29, 1978 which is shown in Figs. 2 and 3. On that day a line of thundershowers formed to the south of the network shortly before 1900 CDT and moved off to the east. However, more intense convective activity was to develop south of Yorkville later that night. And these thunderstorms moved right over the network, causing weak downburst damage in the Yorkville area. Wind speed and direction for each sounding as well as an isotherm analysis are shown in Fig. 2, revealing a fairly well-defined tropopause. As the day progresses, the tropopause becomes even more distinct as warming takes place, intensifying the thermal gradient there. With increased time resolution, the somewhat complicated thermal structure of the lower stratosphere becomes apparent.

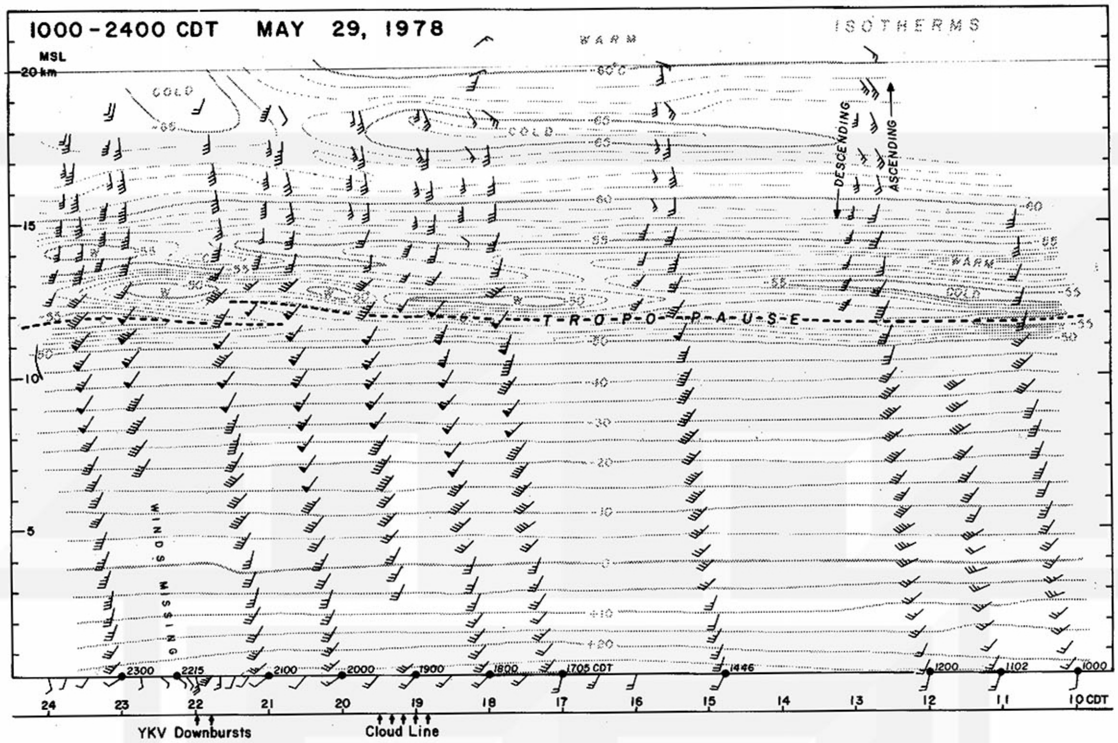

Fig. 2. The serial rawinsonde ascent of May 29, 1978. Wind speed is in knots and isotherms in °C. Notice the lifted tropopause and complicated thermal structure of the lower stratosphere.

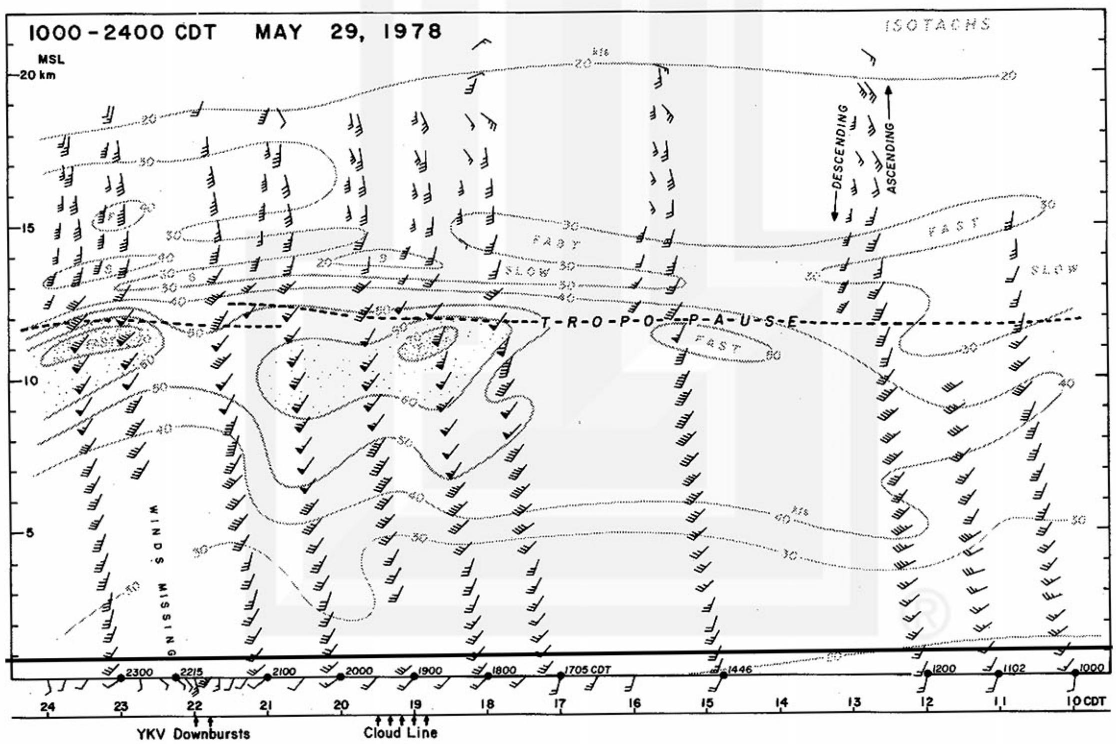

Fig. 3. Isotach analysis for May 29, 1978. Note the wind speed maximum just below the tropopause and the stratospheric easterlies near 20 km.

The isotach analysis in Fig. 3 shows wind speeds that are generally increasing with height to a maximum just below the tropopause. This is consistent with climatology which places the wind speed maximum at tropopause levels. There is a definite increase in this wind maximum to wind speeds of over 70 kts as the thunderstorm outflow modifies the wind field at high levels. Notice the rapid decrease of wind speed with height above the troposphere because the stability of the lower stratosphere serves to limit the vertical extent of tropospheric turbulence (Webb, 1966). The soundings released at 1200, 1446 and 1705 CDT were tracked high enough to enable the detection of stratospheric easterlies at 20 km. In this case, the easterlies are weak because the region is still in transition from its winter circulation to a summertime flow field. Normally, this transition occurs in April or May with the strongest easterlies present later in the summer (Teweles, 1964).

3. STRATOSPHERIC MOISTURE ATOP THE THUNDERSTORM OF JUNE 16, 1978

A number of stratospheric water vapor measurements have been made over the years. Early data collection was undertaken by the British in the 50s, using a frost point hygrometer on aircraft flights into the lowermost stratosphere (Murgatroyd et al., 1955). Another large source of data on moisture in the stratosphere was compiled by the Japanese during the early 60s using dew point measurements taken on radiosonde flights (Hayashi, 1961). The Japanese recorded higher moisture content; however, measurements by Mastenbrook and Dinger (1961) yielded results more in line with what the British had found a decade before. In looking at data obtained during ascent-descent flights, Mastenbrook (1968) showed that spuriously high humidity readings during ascent were caused by moisture contamination in the wake of the flight train.

Another difficulty inherent in radiosonde measurement of stratospheric moisture is the reliability of the carbon film hygristor at low relative humidity and low temperature. An enlargement of a section from a carbon hygristor element is given in Figure 4 showing streaks of carbon embedded in acrylic substrate. Hygristor accuracy was tested at low relative humidity by Brousaides (1975), but testing

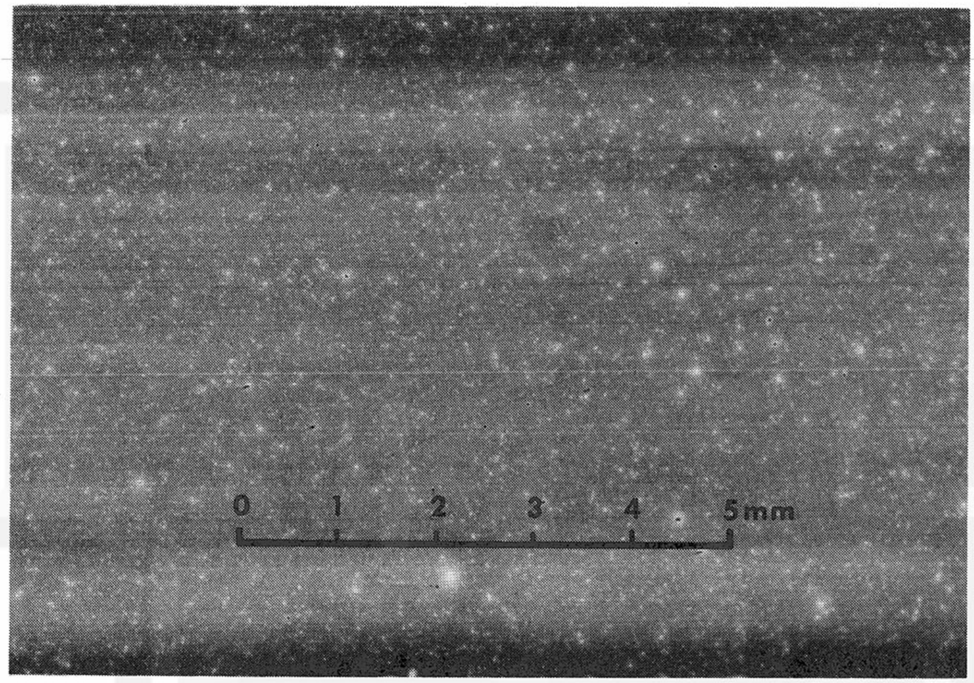

Fig. 4. Enlargement of a section of hygristor element.

was not done below -40°C. The National Weather Service does not compute relative humidity below -40°C and virtually no data exist in the literature to describe the hygristor response at temperatures colder than -40 °C.

These points should be kept in mind when looking at the humidity data collected near the thunderstorm top on June 16, 1978. On that day, a severe thunderstorm moved through the Chicago area during the morning and PAM stations recorded wind gusts in excess of 60 kts. Aerial and ground surveys conducted by the University of Chicago confirmed 3 distinct lines of downburst damage in Chicago's western suburbs. The satellite picture in Fig. 5, taken at 1031 CDT, shows the thunderstorm over the northern third of Illinois. An interesting feature associated with this storm is that streaks of high cirrus are seen protruding from its southern flank. These cirrus fingers are a spectacular result of outflow at upper levels of the storm. By the time this picture was taken the downburst damage had already occurred. A rawinsonde flight was attempted at this time, but the signal was lost soon after the unit entered the storm.

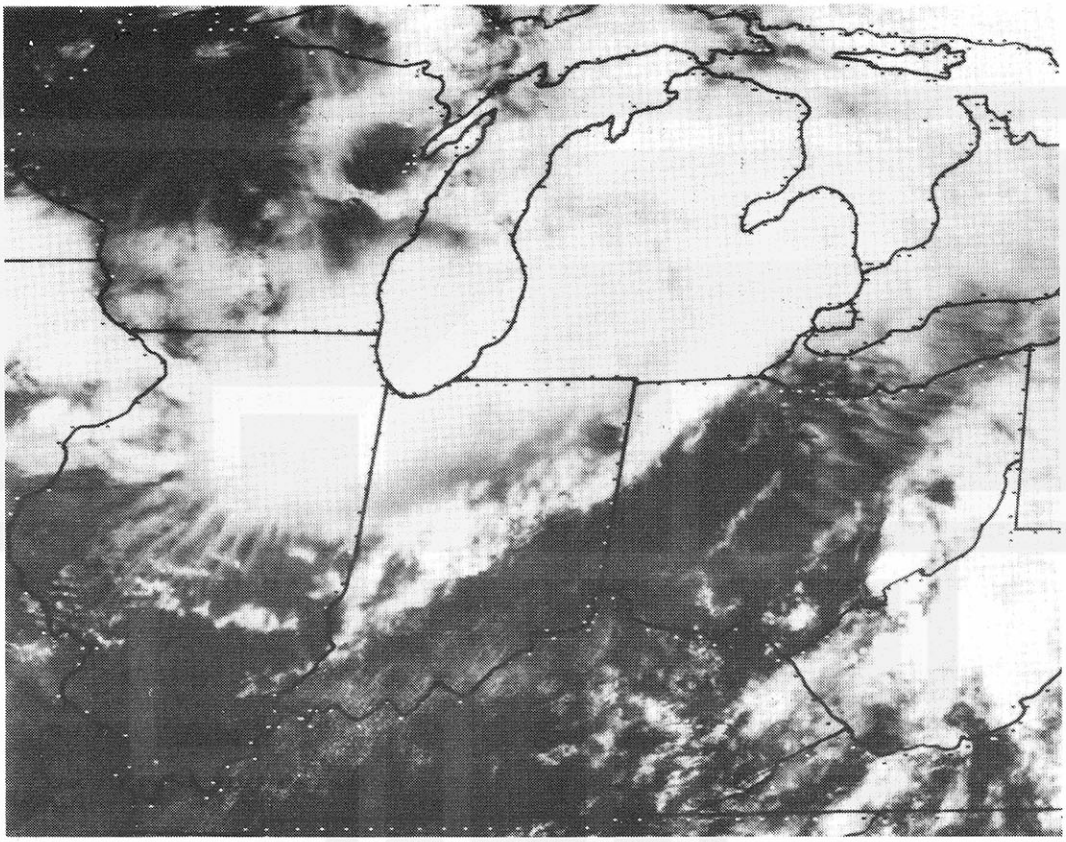

Fig. 5. Satellite picture taken at 1031 CDT on June 16. An intense thunderstorm is located in Northern Illinois with cirrus streaks denoting outflow at the storm top.

Immediately following the storm's passage three successful rawinsonde ascents were made about 60 minutes apart. The position of the three soundings in relation to the thunderstorm is given in Fig. 6. The location of the radiosondes at the tropopause and the time are given in the lower portion of the diagram. Above, a cross-section shows how the radiosondes passed through the storm's western edge. A plot of the temperature sounding is indicated for each release. A vertical distribution of anvil moisture that would be expected from the humidity records for the three soundings is also given. The dotted line above the tropopause delineates the top of the stratospheric region where moisture was detected.

A time-section of the three soundings is given in Fig. 7 showing winds and an isotherm analysis above 400 mb. The tropopause has been significantly lifted by the thunderstorm. A dashed line at 13.5 km for the first sounding, sloping down

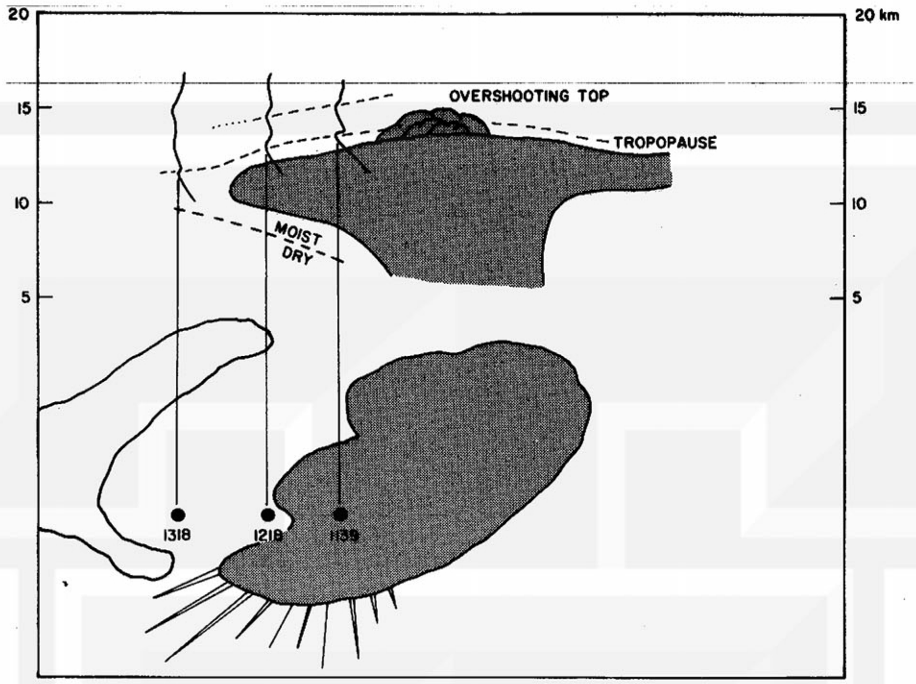

Fig. 6. Schematic diagram of the three soundings in relation to the thunderstorm.

to 12 km at the far left denotes the tropopause. Not only is the tropopause higher on the first sounding, but it is also very sharply defined by a strong temperature gradient. Notice how the cold temperatures at the tropopause moderate as time passes and the storm moves away (Fujita, 1974). Just above the tropopause a region of warmer temperatures exists, while another temperature minimum is detected at 15 km. Again, as before, the maximum wind speeds are found right near the tropopause; however, wind speeds are light in comparison with the winds measured on May 29. Being later in the summer, the stratospheric easterlies are more pronounced. Another interesting feature is the wind shift from NW to WNW near a height of 10 km on the second two soundings. Although not shown in this figure, a similar wind shift was recorded on the first sounding at a height of 7 km.

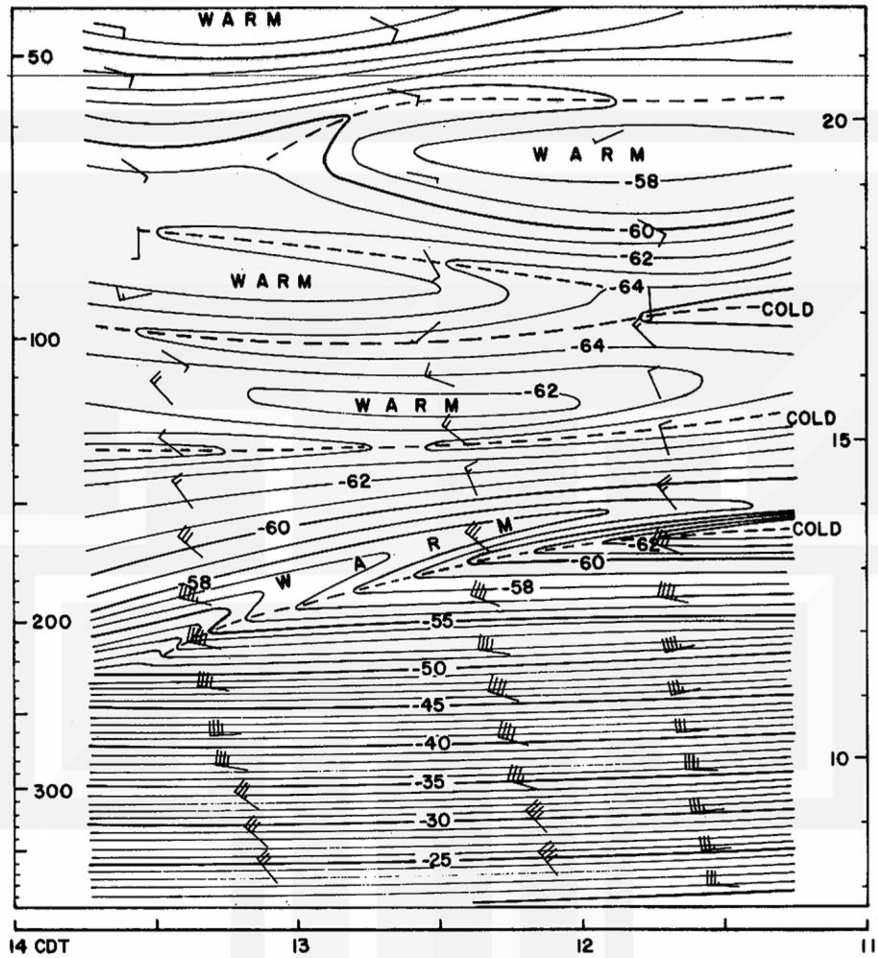

Fig. 7. Isotherm analysis of the soundings taken at 1105, 1140, and 1243 CDT showing the tropopause is lifted near the storm.

The position of the first radiosonde as it crosses into the stratosphere is given on the satellite picture in Fig. 8. Outflow cirrus streaks are still visible along the southern edge of the storm. Further east, more cirrus over eastern Ohio reveals that outflow from this thunderstorm complex is influencing a very large region at upper levels. In Fig. 9 this sounding is plotted above 400 mb. The distance from Yorkville versus height is given in the center of the figure. The distances used in this figure are along the azimuth of maximum radiosonde elevation and can be thought of as projections of the true position onto a plane passing through the Earth's center, Yorkville and the point of balloon burst.

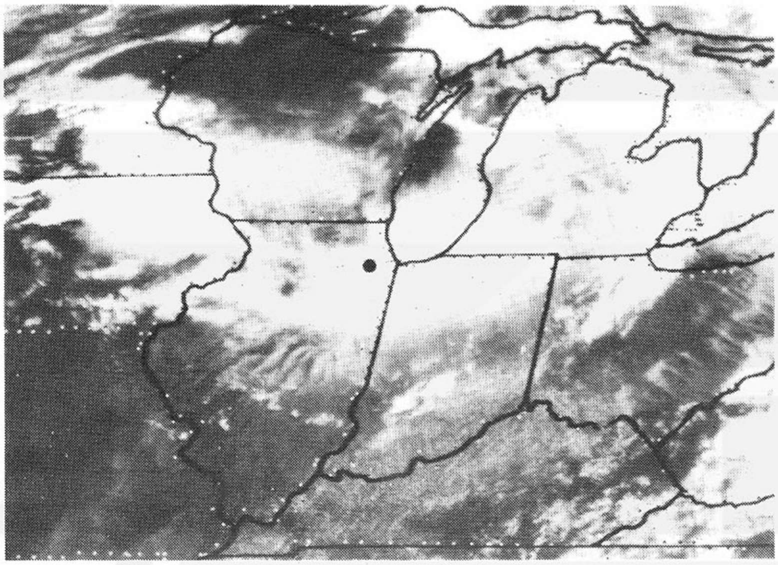

Fig. 8. Position of the 1105 radiosonde at the tropopause. The radiosonde crossed into the stratosphere at 1139 CDT. The time of the picture is 1130 CDT.

The radiosonde's path is under the constant influence of the westerly winds in the troposphere and it steadily moves away from Yorkville. When in the stratosphere, the unit rises almost vertically for 7 km until the balloon finally bursts near 20 km. Due to the easterlies at upper levels of the flight, the radiosonde moves back toward Yorkville, as indicated by the loop in the trajectory. As the unit re-enters the westerlies it proceeds to move off again, away from Yorkville.

The temperature sounding during ascent is shown to the right of the trajectory. The tropopause is very distinct, as seen previously in the isotherm analysis (Fig. 7). Again, the tight gradient just above the tropopause is prominent and a secondary temperature minimum is indicated by the arrow at 125 mb. The relative humidity is shown on the left, revealing humid conditions near 400 mb. Relative humidities in this region are over 70% with respect to water. Nearing the tropopause, the moisture curve levels off to values close to 50%. The humidity discontinuity at the tropopause is very apparent with humidity falling off to near 40% over a short period. Another discontinuity is seen at 15 km, very similar to the humidity tropopause found by Murgatroyd (1955) to exist 2000 to 10,000 ft above the temperature tropopause. This indicates a moist layer above the tropopause is being detected. One should realize that while the absolute value of humidity below -40°C may be erroneous, the tendency is certainly still valid qualitatively.

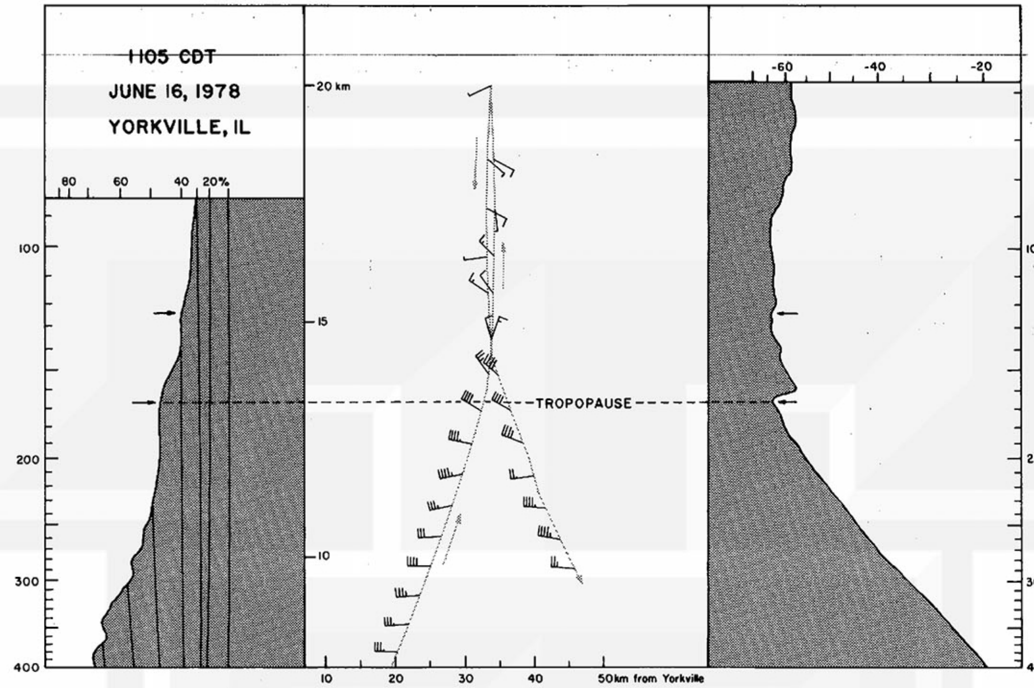

Fig. 9. The 1105 CDT sounding shown above 400 mb. Relative humidity is in % at the left. Rawinsonde position is in the center and temperature in °C is at the right.

The satellite picture taken at 1230 CDT in Fig. 10 shows the storm system moving out of the Chicago area and into Northern Indiana. A dot marks the location of the second radiosonde as it crosses the tropopause. The outflow cirrus streaks have dissipated, although some remnants may still be visible. This sounding is

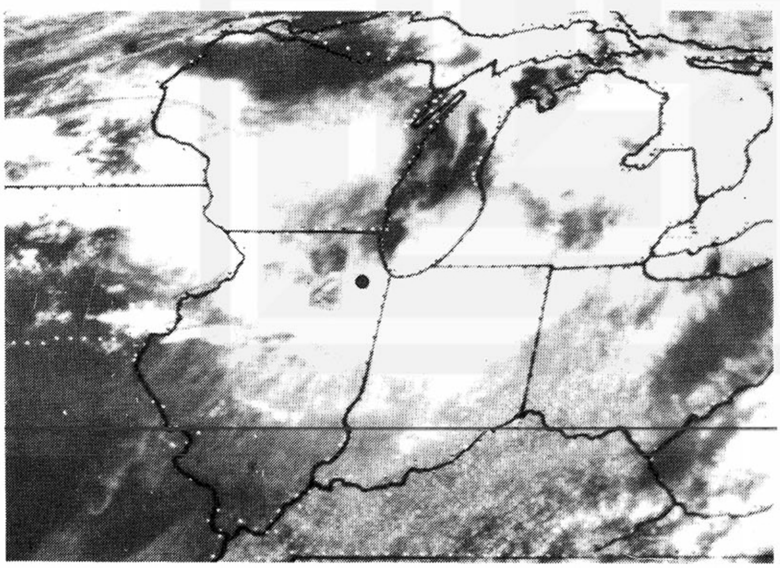

Fig. 10. The 1230 satellite photo shows the storm moving away from Chicago. The radiosonde crosses the tropopause at 1218. The launch time was ~~1140 CDT~~.

plotted in Fig. 11 and again the trajectory shows the same looping seen earlier. This time the loop is accentuated because the flight spent more time under the influence of the easterlies at high levels. As before, the wind speeds are at maximum just

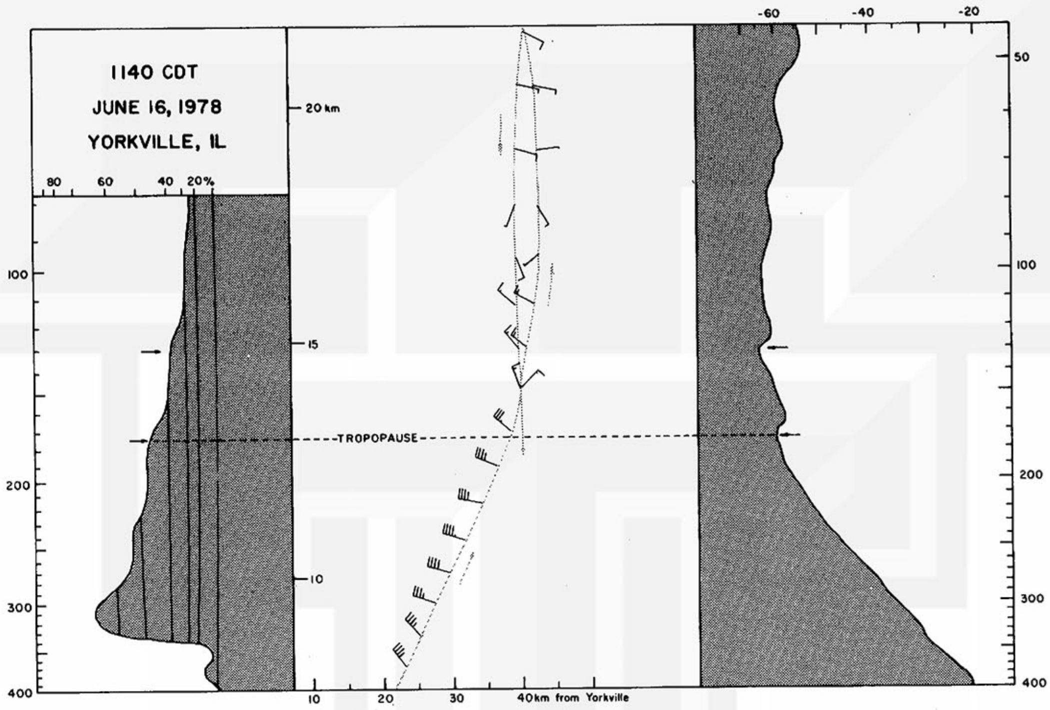

Fig. 11. The 1140 sounding shows humidity dropping off at the tropopause and again at 15 km. The tropopause has become less sharp.

below the tropopause and drop rapidly in the lower stratosphere. The wind shift near the anvil base is seen at 9 km indicating that the anvil base has risen by 2 km since the last sounding. The temperature sounding displays a less distinct inversion at the tropopause with a second minimum near 15 km. From 400 mb to 350 mb the air has dried out considerably with relative humidities on the order of 15%. Notice the sharp rise in moisture near 9 km as the humidity jumps up to almost 70%. This coincides with the NW to WNW wind shift and it seems reasonable that the steep moisture gradient and wind shift are both related to the thunderstorm anvil. The humidity sounding then shows a gradual drop in a series of steplike progressions. As before, the humidity discontinuities at the tropopause and at 15 km are well defined.

The position of the third release is given on the satellite picture in Fig. 12. By this time, the thunderstorm has dissipated over Indiana, leaving a mesohigh over Northeastern Illinois. This satellite picture was taken at 1330 CDT, a full three hours after the thunderstorm was over Chicago. This sounding is very similar to the

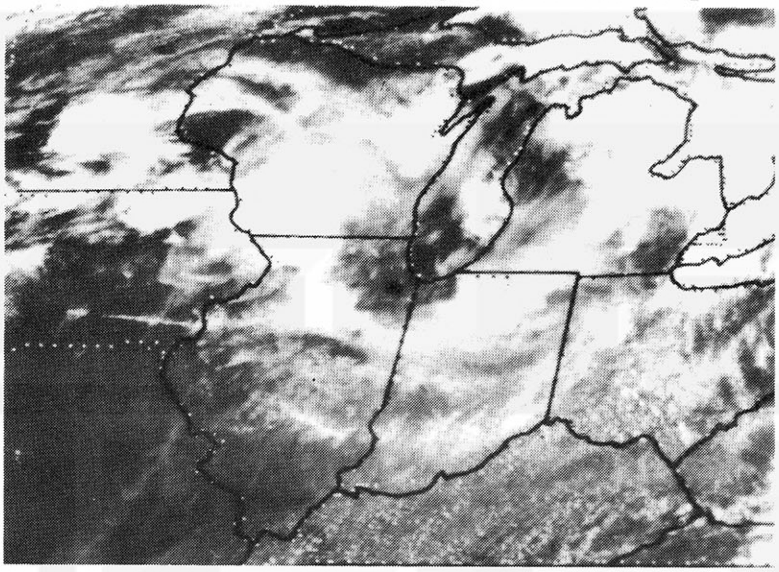

Fig. 12. Balloon position as the 1243 sounding crosses into the stratosphere at 1318. Time of picture is 1330 CDT.

previous sounding with a wind shift and sharp humidity gradient located near 300 mb. Although the radiosonde is in a relatively cloud free region, remnants of anvil moisture are still being picked up. Obviously, the relative humidity is not as high; however, the water vapor is still confined to a distinct layer near the tropopause. The discontinuity in the humidity profile is still evident above the tropopause (Fig. 13).

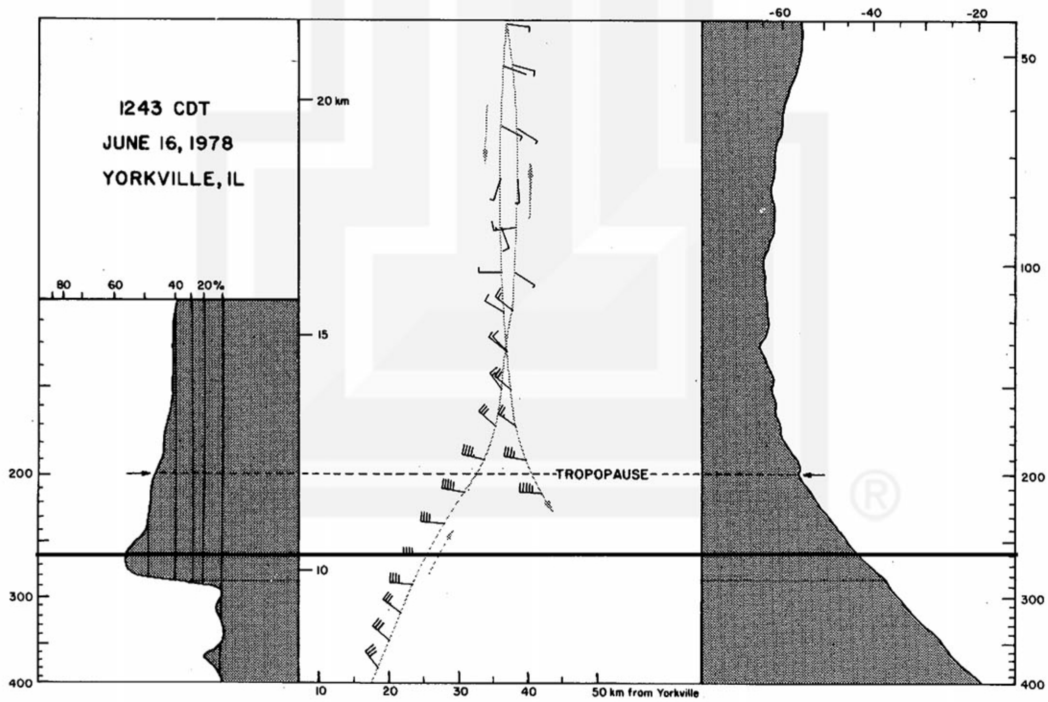

Fig. 13. A plot of the 1243 sounding above 400 mb. The tropopause is less well defined. Notice the stratospheric easterlies at 20 km.

In earlier figures only the ascending records of relative humidity were shown, but the next figure depicts humidity during the ascent and descent for the topmost portion of the first sounding. This serves as a check on the consistency of the humidity record when the up and down portions of the flight are compared. In this format, the humidity fluctuations can be seen as the radiosonde rises through the uppermost troposphere into the stratosphere and back down again.

Humidity ordinate versus time is shown in the upper portion of Fig. 14. The

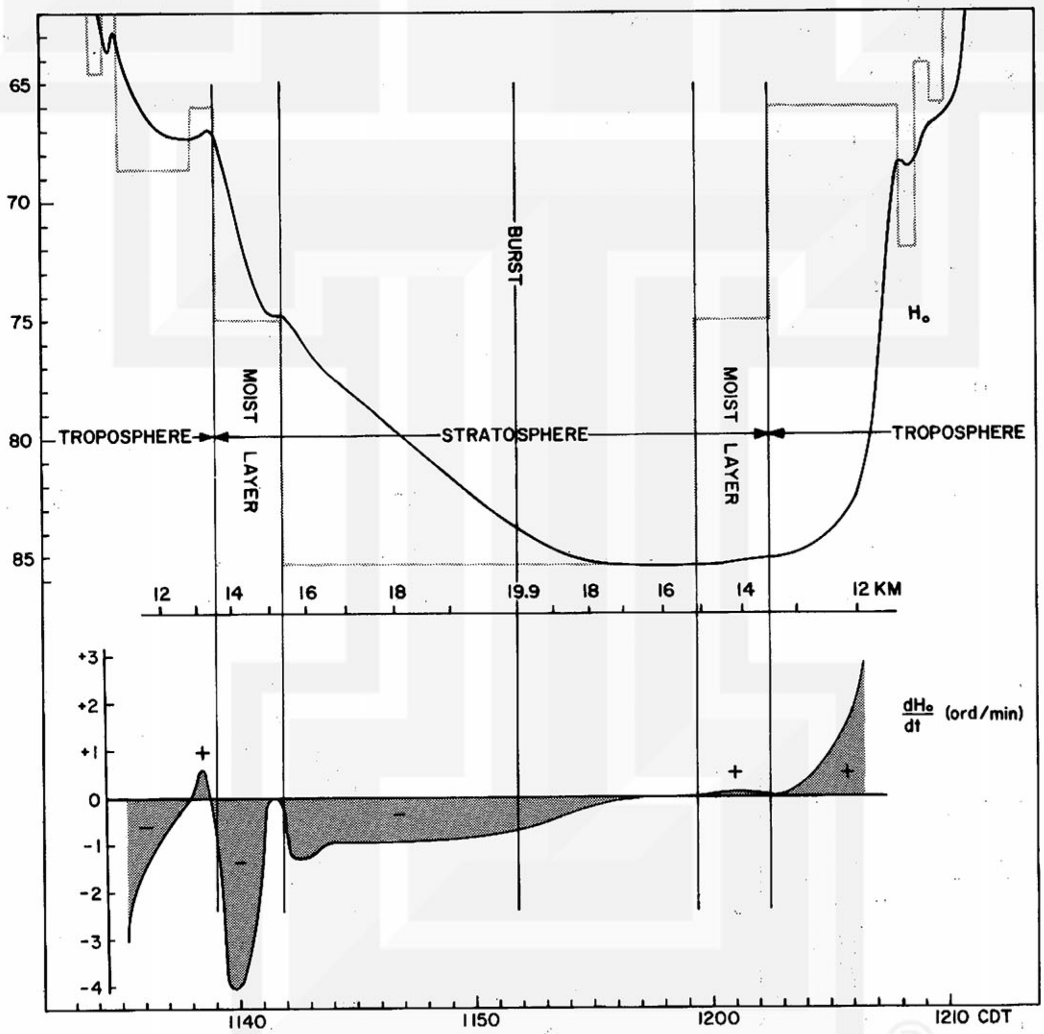

Fig. 14. The 1105 sounding ascending and descending. In the upper portion of the figure humidity ordinate plotted vs. time reveals a moist layer above the tropopause. Time rate of change of humidity ordinate is plotted below.

values of humidity ordinate from the recorder record are functions of temperature and moisture, however, in this ordinate range and low temperature the ordinate values are almost entirely functions of relative humidity alone. High ordinate values coincide with low relative humidity.

At a height of 13.5 km the radiosonde crosses the tropopause at 1139 CDT with the balloon bursting 13 minutes later at 19.9 km. With the parachute deployed, the unit falls back through the tropopause. From this diagram, a general decline of moisture with height can be seen throughout the upper troposphere and lower stratosphere. Just before entering the stratosphere the humidity decline stops and the moisture level increases. Then, there is a rapid drop to a new equilibrium near 15 km as the moist layer above the tropopause is detected. If the hygristor was only detecting the moisture that had been dragged up into the stratosphere, this plateau in the humidity trace would not appear. For the next 13 minutes the radiosonde records a steady decline in humidity as the hygristor comes to equilibrium with the drier stratospheric air. As the radiosonde falls back through the moist layer, a slight but very important rise in the humidity curve can be seen. On the way down, the radiosonde is moving faster so the response is small, however this jump substantiates the fact that the moist layer is real. After reaching the troposphere a rapid rise occurs just below 12 km in response to moisture below the tropopause in the thunderstorm top. Of interest is the fact that this pronounced jump takes place near -55° C, whereas the cutoff temperature for NWS humidity computation is -40° C. Figure 14 also shows the expected moisture distribution in the form of a histogram superimposed on the humidity curve. The rate of change of humidity ordinate with time is also given below the moisture curve. At least in theory, the measured value should equal the actual value when the derivative equals zero.

4. THE OVERSHOOTING PROCESS AND MOISTURE TRANSPORT

A reasonable explanation as to how this moisture is transported across the tropopause is provided by the overshooting and collapsing processes atop severe thunderstorms. Overshooting tops are a frequently-observed characteristic of intense thunderstorms. The overshooting process has been studied from satellite, U-2, and Learjet photography.

In general, the warm stable air of the stratosphere limits the vertical extent of thunderstorm growth; at or near the tropopause, buoyancy becomes neutral and the rising air spreads out forming the characteristic flat anvil top. In thunderstorms with strong updrafts air will be pushed past the level of neutral stability. Because the rising parcel possesses excess kinetic energy it will continue to rise even though it is negatively buoyant. As soon as the kinetic energy is exhausted, the overshooting top, being much colder than the stratospheric environment, collapses (Fujita, 1974). Frequently, anvil cirrus will be thrown up into the stratosphere as the collapsing dome disturbs the anvil cirrus. Stratospheric cirrus was observed by Roach (1966) to "hang around the storm top much like sea spray". Fujita (1975) proposed that as air rushes in behind the collapsing dome it collides, jumping up into the stratosphere, with the jumping height related to the velocity with which the dome sinks. Upon its formation, the jumping cirrus tends to be suspended in the stable stratospheric environment (Umenhofer, 1975). In Fig. 15 jumping cirrus engulfs a collapsing dome.

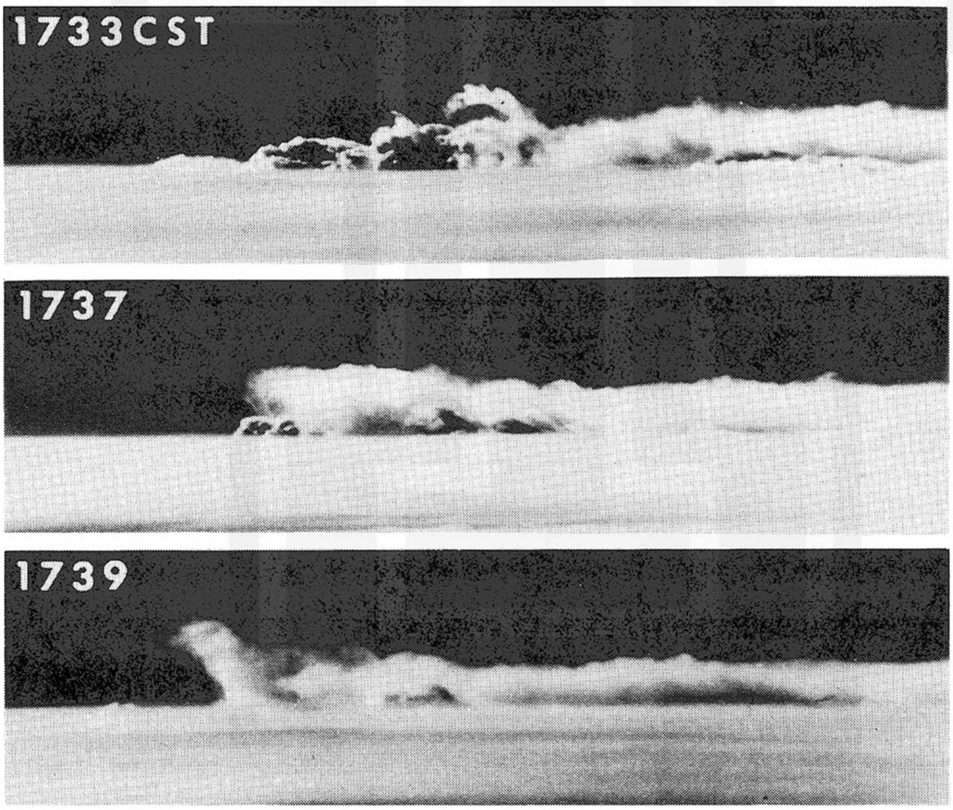

Fig. 15. Jumping cirrus overtakes an overshooting top in the stratosphere. The photo was taken from a Learjet looking north on May 13, 1972. (Fujita, 1974)

The layer of cirrus is estimated to be 2 km deep (Fujita, 1974). On the right, the cirrus is moving toward the east while at higher levels the movement is toward the west. In this way, water vapor is introduced into the stratosphere where it remains as the thunderstorm dissipates and moves away.

5. CONCLUSIONS

This study suggests that the carbon film hygristor responds remarkably well below -40° C and valuable information concerning the moisture distribution at high altitudes can be obtained with serial radiosonde ascents. For a more quantitative look at humidity, using the carbon hygristor at temperatures below -40° C, a better description of the hygristor's response at low temperatures is needed.

A moist layer 2 km deep was detected in the stratosphere, precisely what would be expected from jumping cirrus. Although the jumping cirrus is not visible in the satellite pictures of June 16, it is probable that the overshooting dome collapse and resultant jumping cirrus are responsible for this stratospheric moisture.

ACKNOWLEDGEMENTS

The author would especially like to thank Prof. T. Theodore Fujita for his thoughtful guidance and encouragement. The author also extends his thanks to Gregory Forbes, Duane Stiegler, and Roger Wakimoto for their encouragement and comments regarding this research. The author is also grateful to Jaime Tecson for his work with the rawinsonde computer program. The assistance of Jennifer Cram and Beverly Merrill who diligently reduced the sounding data is greatly appreciated. The author would also like to thank Richard Dreiser for his photographic help in the final preparation of the figures for this paper and Catherine Atkins for the final typing. Finally, the author is most grateful to Tom Adler and Cy Powell of the NWS for the long hours they worked in collecting the NIMROD upper-air data.

Research was performed under NASA Grant No. NGR 14-001-008 and NOAA Grant No. 04-4-158-1.

REFERENCES

Brock, F. V. and P. K. Govind (1977): Portable Automated Mesonet in Operation. J. Appl. Met., 16, 299-310.

Brousaides, F. J. (1975): The Radiosonde Hygristor and Low Relative Humidity Measurements. Bull. Amer. Meteor. Soc., 56, 229-233.

Byers, H. R. and R. R. Braham (1949): "The Thunderstorm." U.S. Government Printing Office, Washington, D. C., 287 pp.

Fankhauser, J. C. (1974): The Derivation of Consistent Fields of Wind and Geopotential Height from Mesoscale Rawinsonde Data. J. Appl. Met., 13, 637-646.

Fujita, T. T. (1974): Overshooting Tops Observed from ATS and Learjet. SMRP Res. Paper 117, Univ. of Chicago, 29 pp.

Fujita, T. T. (1975): Detection of Severe Storms by Satellites. Preprint Vol., 3rd Symposium on Meteorological Observations and Instrumentation, Feb. 10, Washington, D.C., AMS, 5-9.

Hayashi, E. (1961): Distribution of Water Vapor in the Stratosphere by the Dew Point Radiosonde Observation. J. Met. Res., 13, 905-916.

Kreitzberg, C. W. (1968): The Mesoscale Wind Field in an Occlusion. J. Appl. Met., 7, 53-67.

Mastenbrook, H. J. and J. E. Dinger (1961): Distribution of Water Vapor in the Stratosphere. J. Geophys. Res., 66, 1437-1449.

Mastenbrook, H. J. (1968): Water Vapor Distribution in the Stratosphere and High Troposphere. J. Atmos. Sci., 25, 299-311.

Murgatroyd, R. J., P. Goldsmith and W. E. H. Hollings (1955): Some Recent Measurements of Humidity from Aircraft up to Heights of about 50,000 ft over Southern England. Quart. J. Roy. Meteorol. Soc., 81, 533-537.

Roach, W. T. (1967): On the Nature of the Summit Areas of Severe Storms in Oklahoma. Quart. J. Roy. Meteorol. Soc., 93, 318-336.

Teweles, S. (1964): Stratospheric Circulation Studies in the IQSY. Trans. Amer. Geophys. Union, 45, 752-762.

Umenhofer, T. A. (1975): Overshooting Top Behavior of Three Tornado-Producing Thunderstorms. Preprint Vol., Ninth Conf. Severe Local Storms, Oct. 21, Norman, AMS, 96-99.

Webb, W. L. (1966): "Structure of the Stratosphere and Mesosphere." Academic Press, New York, 382 pp.